Frequency Domain Approach for Transonic Aerodynamic Modelling applied to a 3D Wing

Adrien Poncet-Montanges[1], J.E. Cooper[2], D. Jones[3] and A.L. Gaitonde[4]
University of Bristol, Queens Building, University Walk, Bristol, BS8 1TH, UK

Y. Lemmens[5]
Siemens Industry Software, Leuven, Belgium

This work introduces a method for the construction of a reduced order model in the frequency domain. With input data obtained with the TAU linearized frequency domain solver applied to a wing, the reduced order model shows a strong ability to reconstruct the full order frequency response of the lift and pitching moment. Based on a 2D method, the wing is sliced in different strips ; a sensitivity analysis is carried out on each strip and on the total forces and moments to understand the influence of some parameters on the accuracy of the model .

Nomenclature

α	=	angle of attack
α_0	=	amplitude of the pitching motion
α_m	=	mean angle of the pitching motion
C_p	=	pressure coefficient
C_L	=	lift coefficient
C_D	=	Drag coefficient
C_M	=	Pitching moment coefficient
F_z	=	Vertical force
M_Y	=	Pitching moment
k	=	Reduced frequency
U_∞	=	Freestream velocity

I. Introduction

Computational Fluid Dynamics (CFD) now has a wide range of validity where it gives highly accurate results compared to wind tunnel experiments. It is extensively used in industry for steady analysis such as performance studies. However, unsteady aerodynamics also has to be used for aircraft design and aeroelastic applications such as flutter speed or limit cycle oscillation prediction. Whilst more powerful computers have enabled the application of CFD for unsteady loads calculations, in practice the computational cost remains too high for routine use, especially when it comes to viscous flows.

[1] Marie Curie Early Stage Research Fellow in Aircraft Loads. Email : adrien.poncet-montanges@bristol.ac.uk
[2] Royal Academy of Engineering Airbus Sir George White Professor of Aerospace Engineering. AFAIAA.
[3] Senior Lecturer, Department of Aerospace Engineering, University of Bristol, AIAA member.
[4] Senior Lecturer, Department of Aerospace Engineering, University of Bristol, AIAA member
[5] Sr Project Leader RTD, Digital Factory Division, Simulation & Test solutions. Siemens Industry Software.

System identification builds a mathematical description of the dynamic behavior of a system from measured data. The model aims to provide an accurate prediction of the system response for a given input ([1], [2], [3], [4] [5]). Whereas real systems are often costly to describe, models can capture their essential behaviour at reasonable cost. The modelling approach, so called inverse problem [6], consists of determining causes from knowing the effects. This is opposite to a direct problem. As same effects can have different causes, inverse problems may have different solutions. In contrast to direct problems, there is not a unique way of solving them; but a few methods are generally applicable. These inverse problems can be linear (system of equations or integral equation) or non-linear.
Whilst models are useful and can be used to explain data, understand phenomena and predict behaviors; for many of them, a high number of degrees of freedom leads to extended calculation times. Reduced order models (ROMs) can be constructed that aim to decrease the CPU time by capturing the dominant behaviour of the numerical model with a few degrees of freedom, whilst retaining good accuracy and stability. These ROMs enable [7] the study of the system, and establishing control laws to be simplified. Model order reduction can be achieved using different methods; these depend on the physics of the system, the accuracy wanted and the information availability. The latest can be based on physical equations, engineering problems, datasets and so on. For systems whose model is strongly linked to the physics, order reduction can even be performed by hand, thinking about the independencies between the parameters; interpolation can also be used.

While building a ROM, a first technique is to define projection bases and spaces. The idea is to use linear algebra and to construct a subspace orthogonal to the Krylov subspace; this can be performed thanks to the Gram-Schmidt orthonormalization method. Since it can be unstable [8] a modified Gram-Schmidt can be used. In order to achieve this, Arnoldi developed an iterative algorithm [9]. If the system matrix is hermitian, the Lanczos method [10] is much faster. It is based on the Arnoldi method, but as the system matrix is symmetric, the algorithm is much simpler and the recurrence is shorter: each vector U_{j+1} is directly calculated from the two previous ones U_j and U_{j-1}. The Lanczos algorithm can also be combined with a Padé approximation, for a method called Padé via Lanczos (PVL). This method aims to preserve of the stability of the system. In fact, the reduced order modeling techniques using the Padé approximation do not ensure this stability [11]. Other methods such as partial PVL [12] enable the poles and the zeros of the reduced transfer function to be corrected; it leads to an enhanced stability. Antoulas [13] uses the advantages of both Krylov subspaces and balanced truncation approaches. Finally, the Passive Reduced-order Interconnect Macromodelling Algorithm, while using the Arnoldi method guarantees the preservation of passivity and enables an enhanced accuracy [14].

Another stream of scientific analysis uses the system response of different excitations to identify the reduced matrices. Based on Hankel singular values, several algorithms were developed for model reduction such as singular value decomposition (SVD). The idea is to eliminate the states requiring a large amount of energy to be reached, or a large amount of energy to be observed, as both correspond to small eigenvalues [15]. Grammians are introduced since they can be used to quantify these amounts of energy. The reachability grammian quantifies the energy needed to bring a state to a chosen value, whereas the observability grammian quantifies the energy provided by an observed state [16]. The value of these grammians obviously depends on the basis on which they are calculated. In the case of a stable system, a basis in the state space exists in which states that are difficult to reach are also difficult to observe. Normally, the Hankel singular values decrease rapidly. The balanced truncation aims at truncating the modes that are not reachable and observable. They correspond to the smallest Hankel singular values. The singular value decomposition is well-conditioned, stable and can always work, but can be expensive to compute. It solves high-dimensional Lyapunov equations [17] ; the storage required is of the order $O(n^2)$, while the number of operations is of the order $O(n^3)$. Many balancing methods exist, such as stochastic balancing, bounded real balancing, positive real balancing [18]. The frequency weighted balancing [19], can be useful if a good approximation is needed only in a specific frequency range. However, the reduced model is not necessarily stable if both input and output are weighted. These frequency weighted balancing methods have undertaken many improvements: the most recent one guarantees stability and yields to a simple error bound [20]. Based on Markov parameters, the Padé approximation (moment matching method) [21] has then been improved by Arnoldi and Lanczos [10] and is particularly recommended in the case of high dimension systems.

The reduced order model developed in this paper falls into the second category of approach and is described in the following section.

II. Reduced order model

For given flow conditions, the frequency response of the integrated aerodynamic coefficients obtained with a CFD code is directly related to the frequency of the pitching motion. It is therefore appropriate to build a reduced order model of the frequency response in the frequency domain instead of performing a classical reduction in the time domain. After solving the system and transforming back into the continuous space, it is possible to reconstruct any motion in the time domain. The conversion between continuous and discrete spaces (and vice versa) is achieved using a bilinear transform, as it is a bijective function from [0, π] to [0,∞]. The developed method gives accurate results when applied to a pitching airfoil in the transonic range, with no shock-induced separation. It uses the Eigensystem Realization Algorithm [25], based on the singular value decomposition to keep the dominant modes of the frequency response. The method proposed enables a model based on experimental data to be built without knowing the system matrices.

As it needs equispaced input data in the discrete frequency domain, the choice of the sampling spacing is a key element.

The equispaced discrete frequencies are defined by

$$\widehat{\omega}_d(k) = \frac{k\,\pi}{N}, \mathrm{k} \in [0\,, \mathrm{N}] \tag{1}$$

The relationship to continuous frequencies as a result of the linking bilinear transformation is controlled by the sampling time parameter *T* via

$$\omega(\mathrm{k}) = \frac{2}{T}\tan\frac{\widehat{\omega}_d(k)}{2} \tag{2}$$

T has to be chosen such that the continuous reduced frequencies are in the range of interest for the model input. In aerodynamics it corresponds to continuous reduced frequencies mostly in the interval [0.01,10].

A. Singular value decomposition

To map the whole unit circle, the algorithm extends the domain of the input data to the interval [π,2π] using the conjugate of the impulse response coefficients $\mathrm{G_d}$:

$$\mathrm{G}_d(k+N) = \mathrm{G}_d^*(N-k) \tag{3}$$

A singular value decomposition [23] of the Hankel matrix defined using the 2N-points inverse discrete Fourier transform (IDFT) is performed. The model reduction is performed by keeping the largest singular values.

B. Calculation of discrete reduced matrices

A discrete-time linear and stable MIMO model of n-th order, with r-input and m-output can be described using the following state space representation

$$\begin{aligned} \boldsymbol{x}(k+1) &= A_d\boldsymbol{x}(k) + B_d\boldsymbol{u}(k) \\ \boldsymbol{y}(k) &= C_d\boldsymbol{y}(k) + D_d\boldsymbol{u}(k) \end{aligned} \tag{4}$$

$\boldsymbol{x}(t) \in \mathbb{R}^{\mathrm{n}}$ represents the vector of different degrees of freedom (called state vector in control theory). It contains for example the unknown physical variables, such as velocity, pressure, density. $\boldsymbol{y}(t) \in \mathbb{R}^{\mathrm{p}}$ and $\boldsymbol{u}(t) \in \mathbb{R}^{\mathrm{m}}$ respectively represent the vector of the outputs of interest of the system, and the vector of inputs. Another convenient notation is also used for a discrete-time model:

$$G_d : \begin{pmatrix} A_d & B_d \\ C_d & D_d \end{pmatrix} \tag{5}$$

As far as a continuous-time is concerned, the matrices are written in this paper under the form

$$G : \begin{pmatrix} A & B \\ C & D \end{pmatrix} \tag{6}$$

The reduced matrices $\hat{A}_r$ and $\hat{C}_r$ are calculated [24]. G can be written as

$$\widehat{G_d} = \hat{C}_d(zI - \hat{A}_d)^{-1}\hat{B}_d + \widehat{D}_d, z \in \mathbb{C} \tag{7}$$

The calculation of $\hat{B}_r$ and $\widehat{D}_r$ is achieved by decomposing G in its real and imaginary parts.

C. Bilinear transformation

G can be transformed in a discrete-time system

$$\hat{G}_d(z) = \widehat{D}_d + \hat{C}_d(zI - \hat{A}_d)^{-1}\hat{B}_d \tag{8}$$

using the bilinear transformation [25]:

$$\hat{A} = \frac{2}{T}\,(I + \hat{A}_d)^{-1}\,(\hat{A}_d - I) \tag{9}$$

$$\hat{B} = \frac{2}{\sqrt{T}}(I + \hat{A}_d)\,\hat{B}_d \tag{10}$$

$$\hat{C} = \frac{2}{\sqrt{T}}\,\hat{C}_d\,(I + \hat{A}_d)^{-1} \tag{11}$$

$$\widehat{D} = \widehat{D}_d - \hat{C}_d\,(I + \hat{A}_d)^{-1}\,\hat{B}_d \tag{12}$$

III. Test case introduction : FFAST wing

A. Static results, FFAST wing

As it gives promising results when applied to an airfoil ([26]), this model is applied to a wing in a pitching motion. The wing chosen is the one used for the FFAST project ([27]), as it is a case of interest in the framework of ALPES (Aircraft Loads Prediction using Enhanced Simulation). To be able to use CFD, a mesh is created for inviscid simulations with TAU [28].

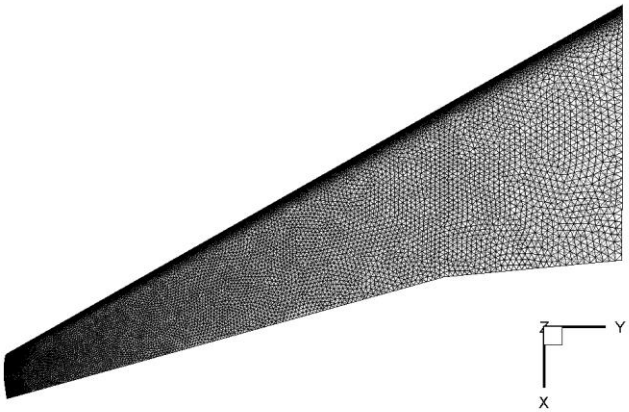

Figure 1: Euler mesh, FFAST wing

The freestreams conditions are :

Mach =0.85
Reference temperature = 216.65 K
Reference density = 0.365
α_m *= 2 degrees*

The solver uses central discretization, a scalar dissipation scheme, and the chosen relaxation solver is Runge Kutta. The convergence is reached for every calculation performed in the following part.
The static lift and pitching moment show a linear trend as a function of the angle of attack (Figure 2)

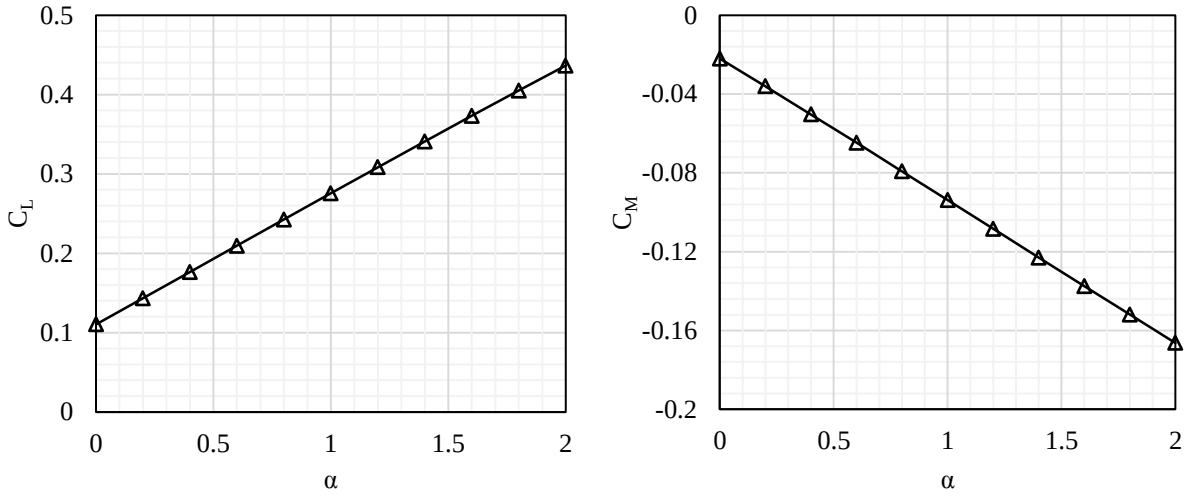

Figure 2: Static C_L and C_M vs α

To have a better of the aerodynamics on the wing, the C_p and the Mach number are plotted on the upper surface at α_m = 2 degrees (Figure 3).

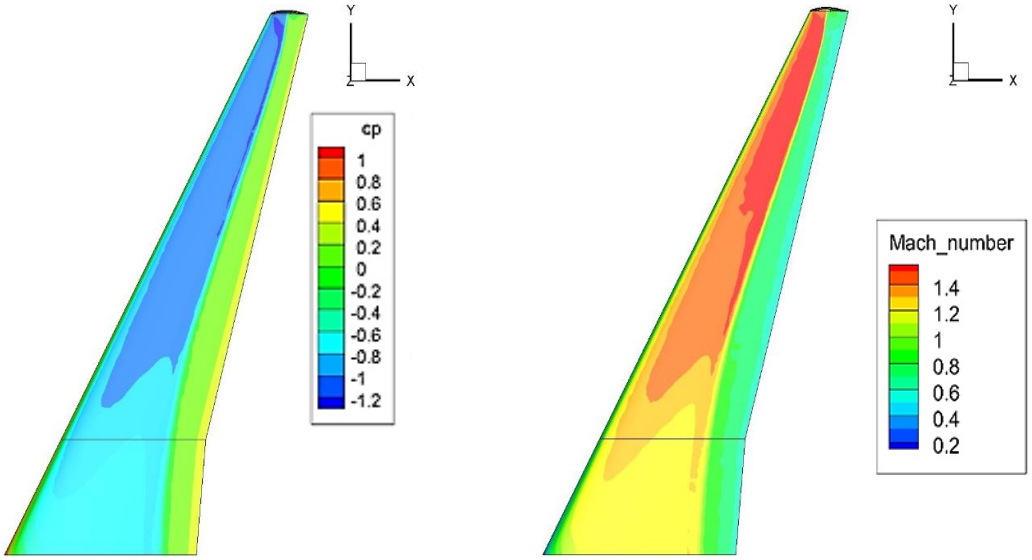

Figure 3: Static C_p and Mach number, α_m = 2 degrees

It displays at standard evolution for the C_p and Mach number, with the strongest shock reached around 70% chord.

B. Unsteady aerodynamics

The motion is sinusoidal and described by the following equation:

$$\alpha = \alpha_m + \alpha_0 \cdot \sin(\omega \cdot t) \tag{13}$$

where α_m is the mean angle of attack, α_0 the amplitude and ω the frequency of the motion. Let U_∞ be the freestream velocity and c the airfoil chord, the reduced frequency is defined such as

$$k = \frac{\omega \cdot c}{U_\infty} \tag{14}$$

In addition to the classical unsteady Euler computations, as the amplitude of the motion is small and the motion periodic, it is possible to use the linearized frequency domain solver [29].

C. Linearized frequency domain solver

In addition to the classical Euler computation, as the amplitude of the motion is small and the motion periodic, it is possible to use the linearized frequency domain solver [27].
An unsteady governing equation of the fluid motion discretized in space can be written

$$\frac{d\boldsymbol{u}}{dt} + R(\boldsymbol{u}, \boldsymbol{x}, \dot{\boldsymbol{x}}) = 0 \tag{15}$$

where R is the residual, written as a function of the flow solution u, the grid coordinates x and the grid velocities $\dot{x}$. Under the assumption of a small amplitude of the unsteady perturbations, the RANS equation can be linearized around the steady state, i.e. it is seen as the superposition of the steady state mean and of the perturbation.

$$\boldsymbol{u}(t) = \bar{\boldsymbol{u}} + \tilde{\boldsymbol{u}}(t)\,, \qquad \|\tilde{\boldsymbol{u}}\| \ll \|\bar{\boldsymbol{u}}\| \tag{16}$$

$$\boldsymbol{x}(t) = \bar{\boldsymbol{x}} + \tilde{\boldsymbol{x}}(t), \qquad \|\tilde{\boldsymbol{x}}\| \ll \|\bar{\boldsymbol{x}}\| \tag{17}$$

and transformed in the frequency domain, since the perturbation is assumed to be periodic and can expressed as

$$\tilde{x}_k(t) = \sum_k Re(\hat{x}_k\, e^{jk\omega t}) \tag{18}$$

where $\hat{x}_k$ are the complex Fourier coefficients of the motion, ω the frequency, k the mode and j complex number such as

$$j = \sqrt{-1} \tag{19}$$

After replacing the linearized values of u(t) and x(t) in (**Error! Reference source not found.**), the following system is obtained

$$A\boldsymbol{x} = b \; where \; A = \begin{pmatrix} \frac{\partial R}{\partial u} & -\omega I \\ \omega I & \frac{\partial R}{\partial u} \end{pmatrix}, b = \begin{pmatrix} \frac{\partial R}{\partial x} & -\omega \frac{\partial R}{\partial \dot{x}} \\ \omega \frac{\partial R}{\partial \dot{x}} & \frac{\partial R}{\partial x} \end{pmatrix} \begin{pmatrix} \tilde{x}_{Re} \\ \tilde{x}_{Im} \end{pmatrix} \tag{20}$$

The Jacobian $\partial R/\partial u$ is theoretically calculated in TAU, but the right hand term is evaluated by using central finite differences

A comparison is made between the magnitude and phase of lift and moment obtained by the LFD solver and the one given by a standard time domain simulation. The harmonics of lift and moment are the main output of the LFD solver. In the case of the time domain simulation, the harmonics are calculated by TAU at the end of each period of the pitching motion. However, it is necessary to wait a few periods so that the values of the harmonics are converged.

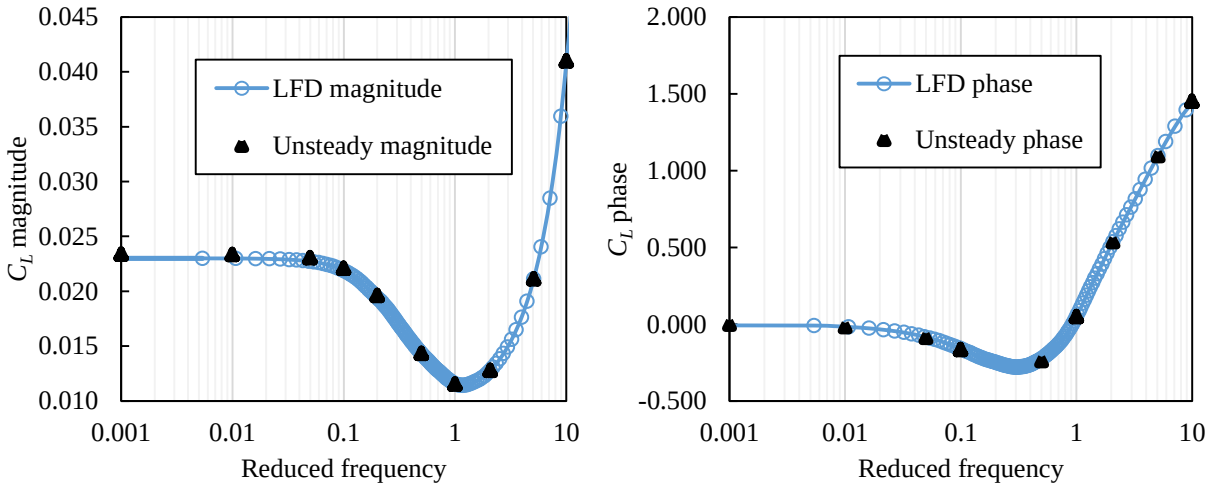

Figure 4: LFD vs time domain simulation, lift, FFAST wing

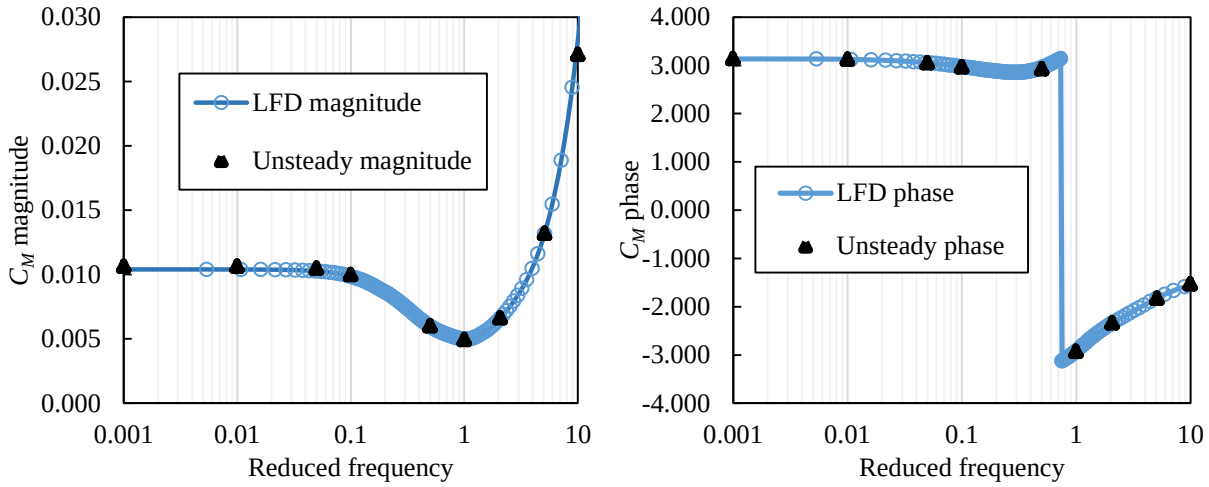

Figure 5: LFD vs time domain simulation, pitching moment, FFAST wing

After having proved its efficiency to estimate the lift and the pitching moment in the case of a pitching airfoil, the linear frequency domain solver shows a good accuracy when estimating the loads on a wing (Figure 4-5), in a fast calculation time, compared to a time domain simulation.

D. Slicing the surface mesh

To effectively model the aerodynamic coefficients on the wing, the surface mesh is sliced in parts (Figure 6).

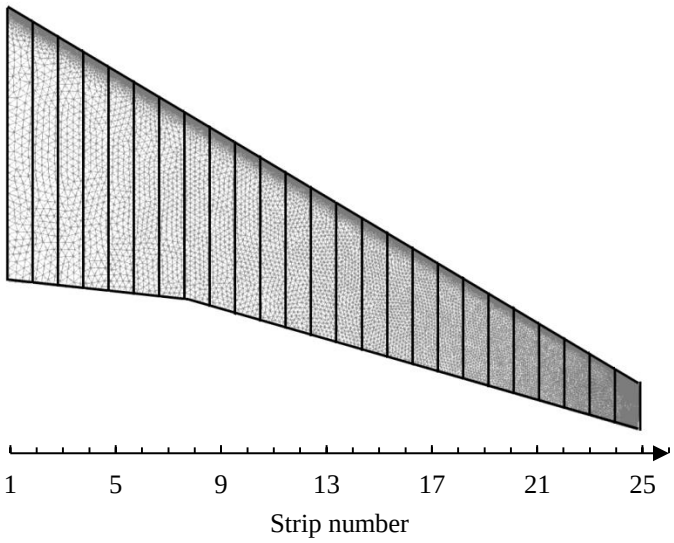

Figure 6: Definition of the strip numbers

A LFD calculation is launched for each reduced frequency wanted. TAU outputs a solution file containing the position of the nodes of the surface mesh, with the real and imaginary parts of C_p and C_f for each node. A script developed by Chris Wales at the University of Bristol enables the user to choose the number of strips he wants, and their position. For each strip, it extracts from the solution the position of the nodes, before sorting the triangular or

quadrilateral elements depending if they are contained in this strip or at its boundary. It uses the TAU solution file to extract the pressure coefficient (and the friction coefficient if desired) for each element, with a clever approach for the elements on the boundary ; it can then easily calculate the total pressure and moment on each strip. In the case of the LFD solver, the outputs given by TAU on the the surface are Re(C_p) and Im(C_p), giving Re(F_Z), Im(F_Z), Re(M_Y) and Im(M_Y). F_Z magnitude and phase can then be calculated, the same approach being valid for the pitching moment.

$$abs(F_Z) = \sqrt{Re(F_Z)^2 + Im(F_Z)^2} \tag{21}$$

$$arg(F_Z) = arctan\left(\frac{Im(F_Z)}{Re(F_Z)}\right) \tag{22}$$

LFD calculations are launched at different frequencies, and at each frequency, the script detailed above is used to give the real and imaginary parts of the aerodynamic coefficients. It enables to plot these coefficients against the wingspan at different frequencies. The arrow represents the increasing values of reduced frequency.

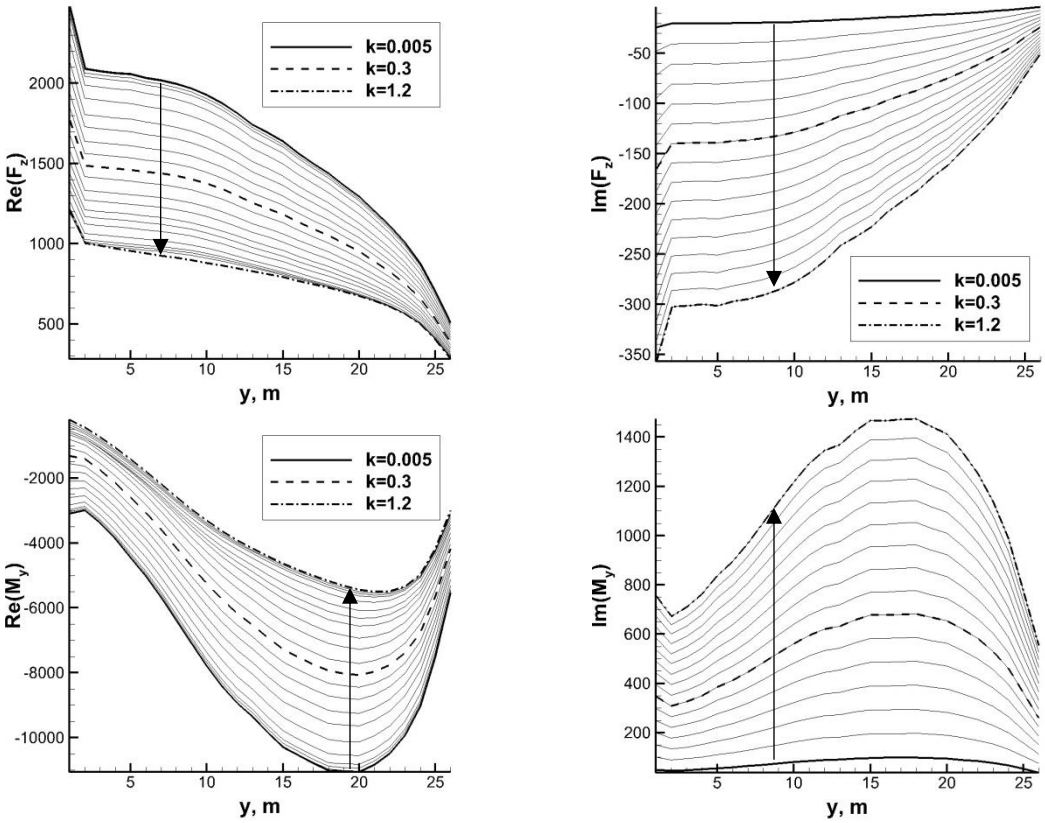

Figure 7: Re(F_Z), Im(F_Z), Re(M_Y), Im(M_Y) vs wingspan

Re(F_Z)) shows the typical distribution of the vertical force on a wing, and both values of Re(F_Z) and Im(F_Z) decrease with the reduced frequency. As far as the moment is concerned, Re(M_Y) reaches a minimum around y=19, where Im(M_Y) reaches a maximum, which is due to the shock strength in this region (Figure 3).

As it has been specified before, the wing is sliced in 25 strips, Strip 1 being the strip close to the fuselage, and Strip 25 the wingtip. The aim is to build a reduced order model for the lift and the pitching moment on each strips. First, for different strips (1, 5, 10, 15, 25) the magnitude and the phase of F_Z is plotted as a function of the reduced frequency. It enables to have a better idea of the behavior of these two values depending on the position of the strips along the wing (Figure 8).

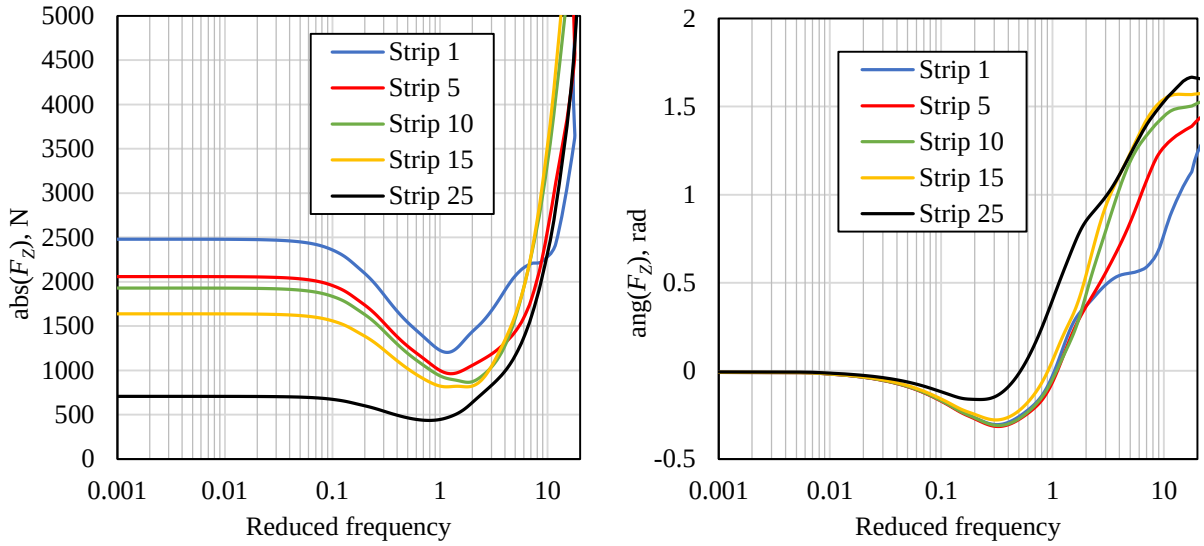

Figure 8: abs(F_Z), ang(F_Z) vs reduced frequency, different strips

Different trends are observed as far as the magnitude is concerned, especially for Strip 1 that shows one more inflexion point than the others. It may then be harder to build a reduced order model of Strip 1 than to build a ROM of Strip 25, for example.

E. Building the reduced order models : process

The reference set of data consists of 128 LFD calculations at different frequencies. Due to the choice of the method used to build the ROM, the mapping of these frequencies is driven by the spacing of the bilinear transform. As written in (2), the data has to be equispaced in discrete time.

T has to be chosen such that the continuous reduced frequencies are in the range of interest of the model input. In aerodynamics it corresponds to continuous reduced frequencies mostly in the interval [0.01,10]. Three different values will be tried : T=0.005, T=0.02, and T=0.08.

Moreover, the model can be used to reconstruct the frequency response G_r on a chosen number N_r of equispaced discrete frequencies corresponding to the same number of continuous frequencies. The reference set of inputs is built with 128 inputs, but it is interesting to see how the accuracy of the prediction changes when this number of input decreases. Models will be built with N=128, N=64, N=32 and N=16.

The process is represented on Figure 9.

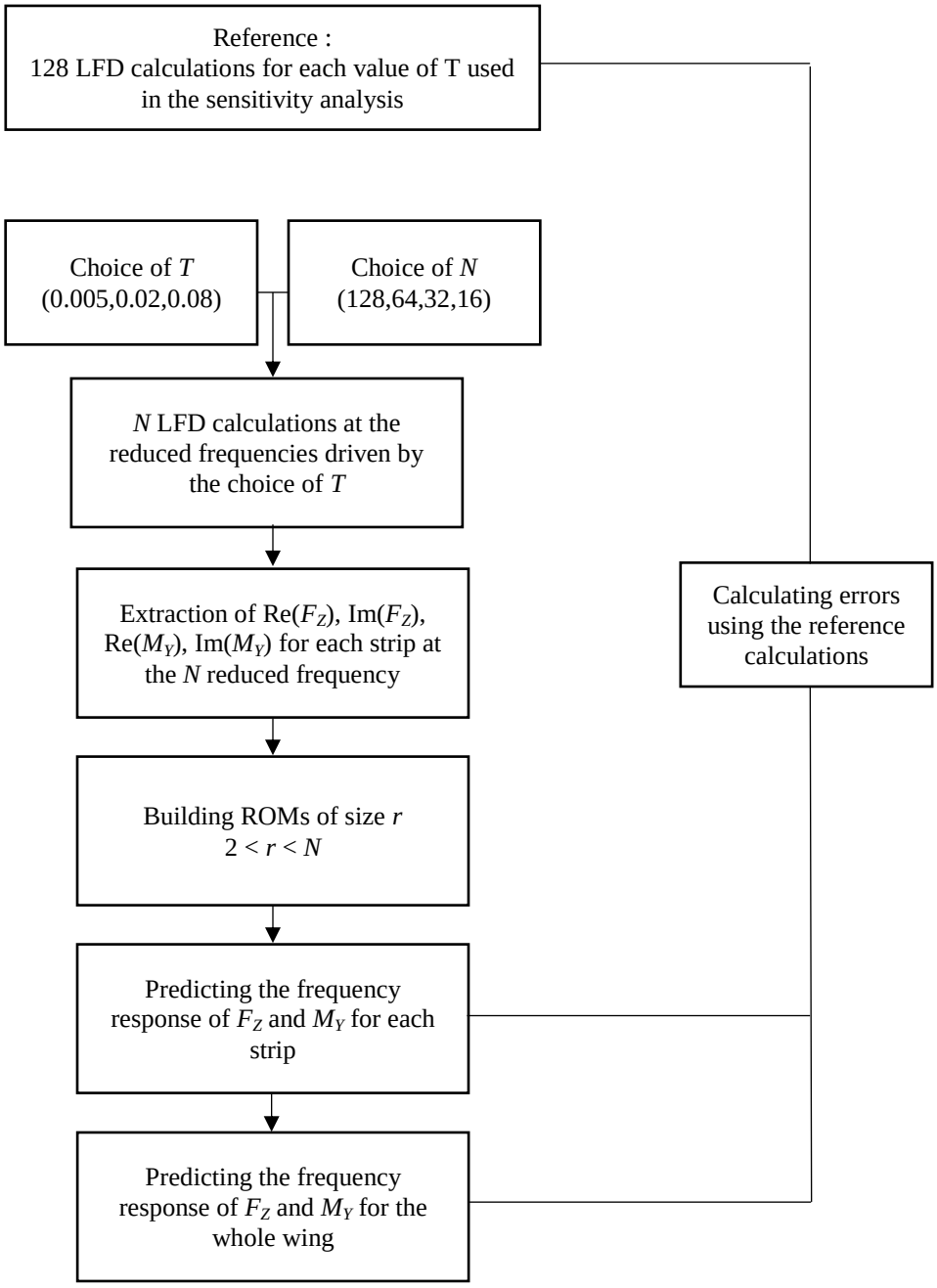

Figure 9: Description of the process

IV. Results

A. Results strip by strip, influence of the choice of *T* and *N*

Three different spacings are chosen for the bilinear transform. Each value of *T* gives a different mapping of continuous frequencies against the discrete frequency (Figure 10).

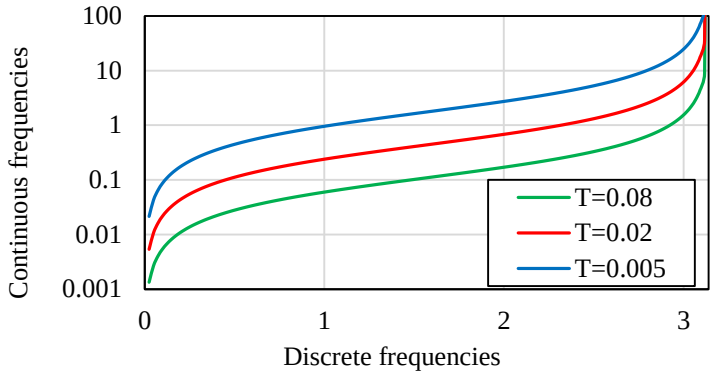

Figure 10: Choice of *T* for the sensitivity analysis

T=0.08 contains more information on the low frequencies whereas *T*=0.005 contains more information on the high frequencies. To calculate errors for a given value of *N*, the ROM outputs its prediction at each point where there is a LFD calculation used as the reference. The relative error between the prediction is then calculated (23).

$$Relative\ error\ = \frac{|Refererence_{\ LFD} - Prediction_{ROM}|}{Refererence_{\ LFD}} * 100 \tag{23}$$

The first test case focuses on Strip 1, with *r*=9, and *N*=16 or *N*=32. As *T* has a direct impact on the mapping of the input with the reduced frequency, the relative error in vertical force magnitude is plotted against *k* (Figure 11).

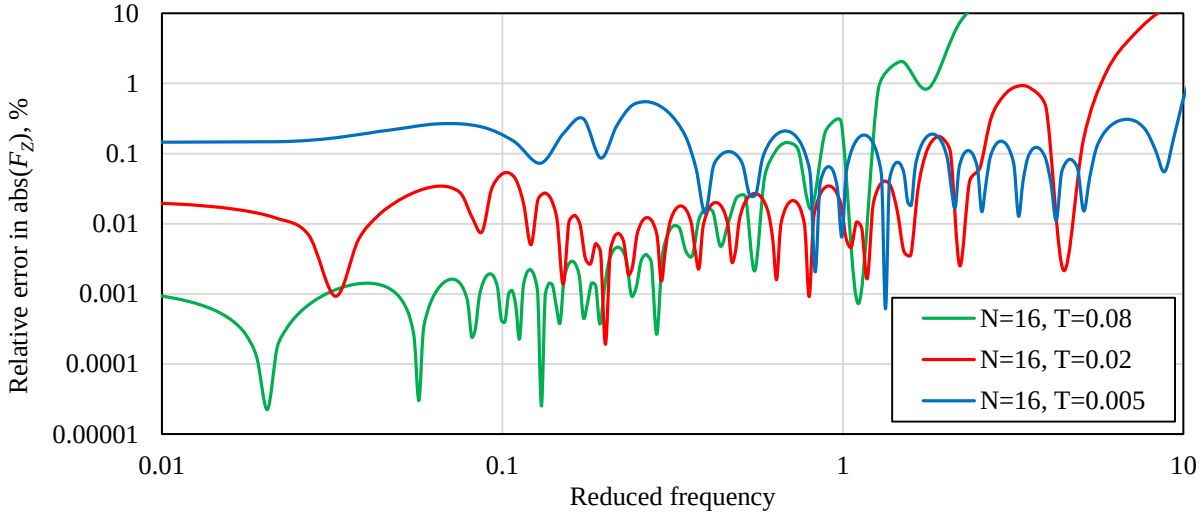

Figure 11: Relative error in F_Z magnitude vs *k*, influence of T. Strip 1, *r*=9, *N*=16

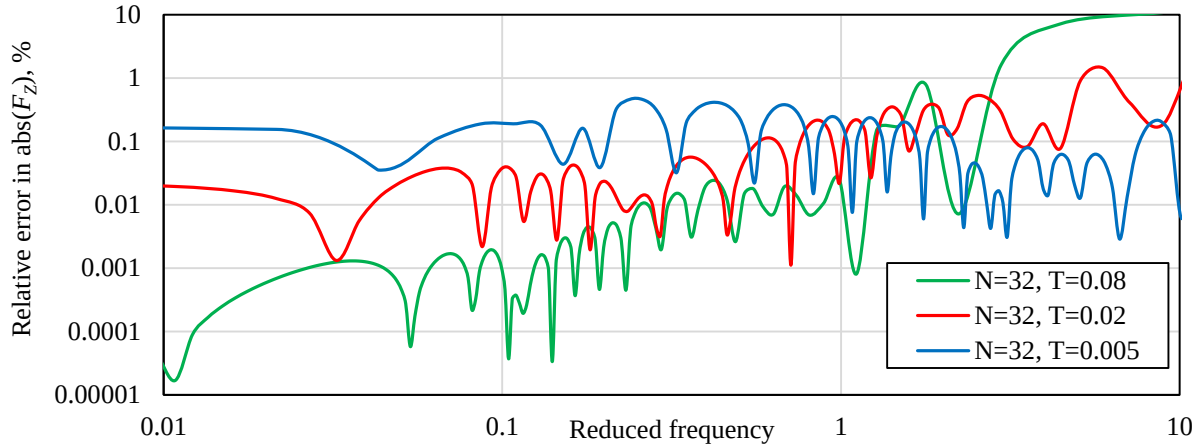

Figure 12: Relative error in F_Z magnitude vs k, influence of T. Strip 1, r=9

As expected since as the inputs are mainly in the low frequencies (Figure 11-12), T=0.08 gives a good accuracy for low frequencies compared to the other values of T. However, the prediction is bad for high frequencies (for $1 < k < 10$) : the error in F_Z magnitude reaches 10% in this frequency range, which is not satisfactory. As far as T=0.005 is concerned, this is the opposite ; small error for high frequencies, but high error for low frequencies. T=0.02 seems to be a good trade-off and seems to guarantee a good accuracy for the whole range of frequencies.

To be able to have on overview of the trend of the errors depending on the ROM size, the mean absolute percentage error (MAPE) is calculated. For each ROM size, it actually represents the averaged sum of the relative errors at the 128 reduced frequencies.

$$MAPE = \frac{1}{128} \sum_{k=k_1}^{k=k_{128}} \frac{|Refererence_{\ LFD} - Prediction_{ROM}|}{Refererence_{\ LFD}} * 100 \qquad (24)$$

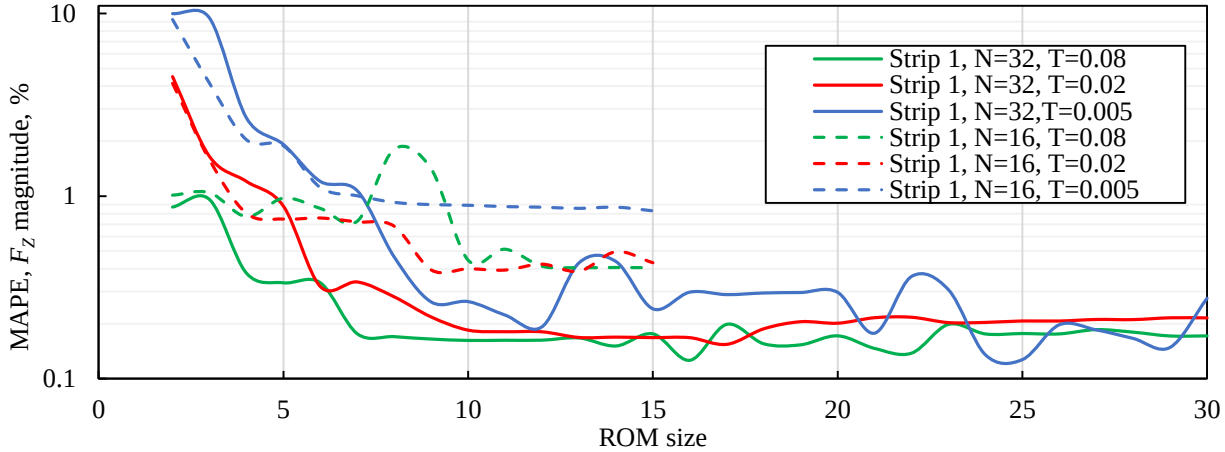

Figure 13: Mean absolute percentage error vs ROM size on Strip 1, F_Z magnitude

For N=16, the MAP error given by T=0.005 does not go below 1% and the best result is obtained for T=0.02. When using 32 inputs, T=0.02 and T=0.08 give similar results. As a conclusion, focusing on Strip 1 enables to say that choosing T=0.005 does not provide a good accuracy.

It is necessary to have a general look on the MAP error for all the strips. The number of inputs chosen is N=32. For each value of T, and for each strip, the mean absolute percentage error is plotted as a function of the ROM size.
The strips can be identified thanks to a color gradient. From strip 1 to strip 25, the MAPE error value is represented from a dark to a light color (Figure 14).

Moreover, on each graph, the average MAPE is represented by a black line, enabling an easier analysis.

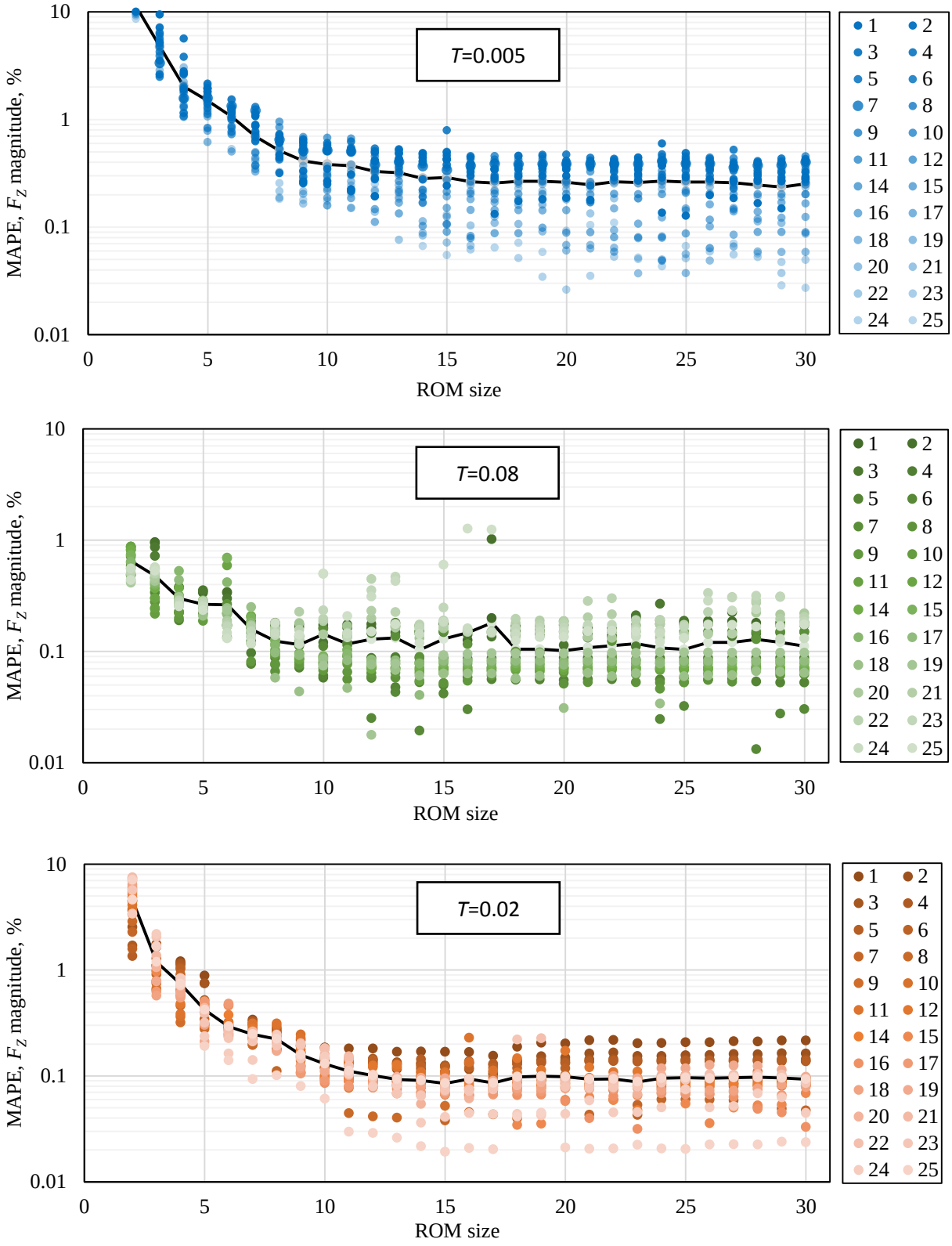

Figure 14: MAPE vs ROM size, F_Z magnitude, N=32

The error in F_Z magnitude with T=0.005 tends to an average MAPE of 0.3% for r=15, whereas T=0.02 and T=0.08 give an average MAPE of 0.1%. Nevertheless, in the case T=0.08, the error locally reaches 1% ; T=0.02 gives a much smoother plot, so this value will be kept for the following part. Finally, once the value of T has been set to 0.02, a last comparison is done for the average MAPE against the ROM size, for different numbers of inputs (Figure 15).

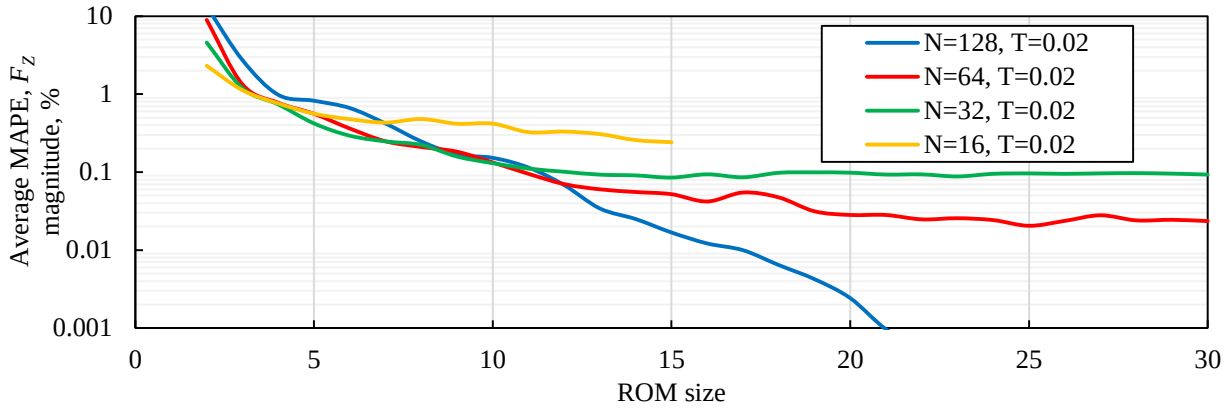

Figure 15: Average MAPE vs ROM size, F_Z magnitude, T=0.02

When using 128 inputs, the average MAP error on all strips gets really low and reaches 10^{-5} %. A good trade-off is given for N=32, the error reaching 0.1% in average in this case. This sensitivity study has shown that choosing N=32 and T=0.02 enables to build efficient and accurate ROMs.

B. Total forces and moments on the wing

Once that a ROM has been built for each slices, the total force on the wing is given by the sum of the forces on each slices. With N=32 and T=0.02, and for $0.01 < k < 1$, the error of prediction of the total force on the wing is around 1% for a ROM of size 3, 0.1% for r=9, and 0.0001% for r=15 (Figure 16).

As far as high frequencies are concerned for r=15, the relative error does not exceed 0.1%. This increase in error is due to the low number of inputs in this range. However, a maximum error lower than 0.1% guarantees a very good accuracy. Increasing the size of the ROM does not increase the accuracy for r >15. It confirms what has been observed when checking the accuracy of the ROM strip by strip : for a given N and T, the best prediction is already obtained when r=15, which is a reasonable size.

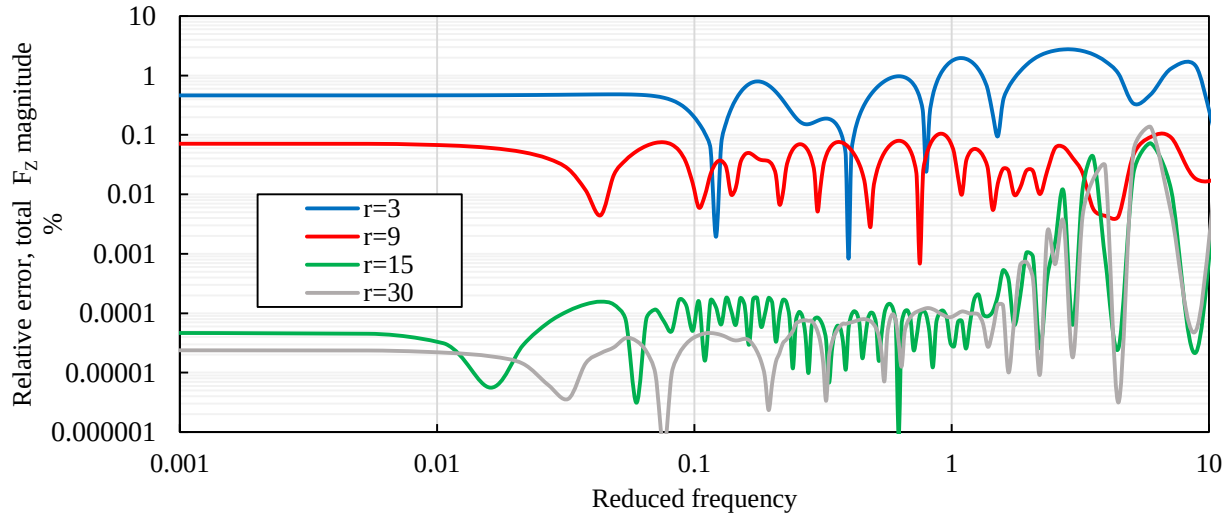

Figure 16: Relative error in total F_Z magnitude vs ROM size, T=0.02, N=32

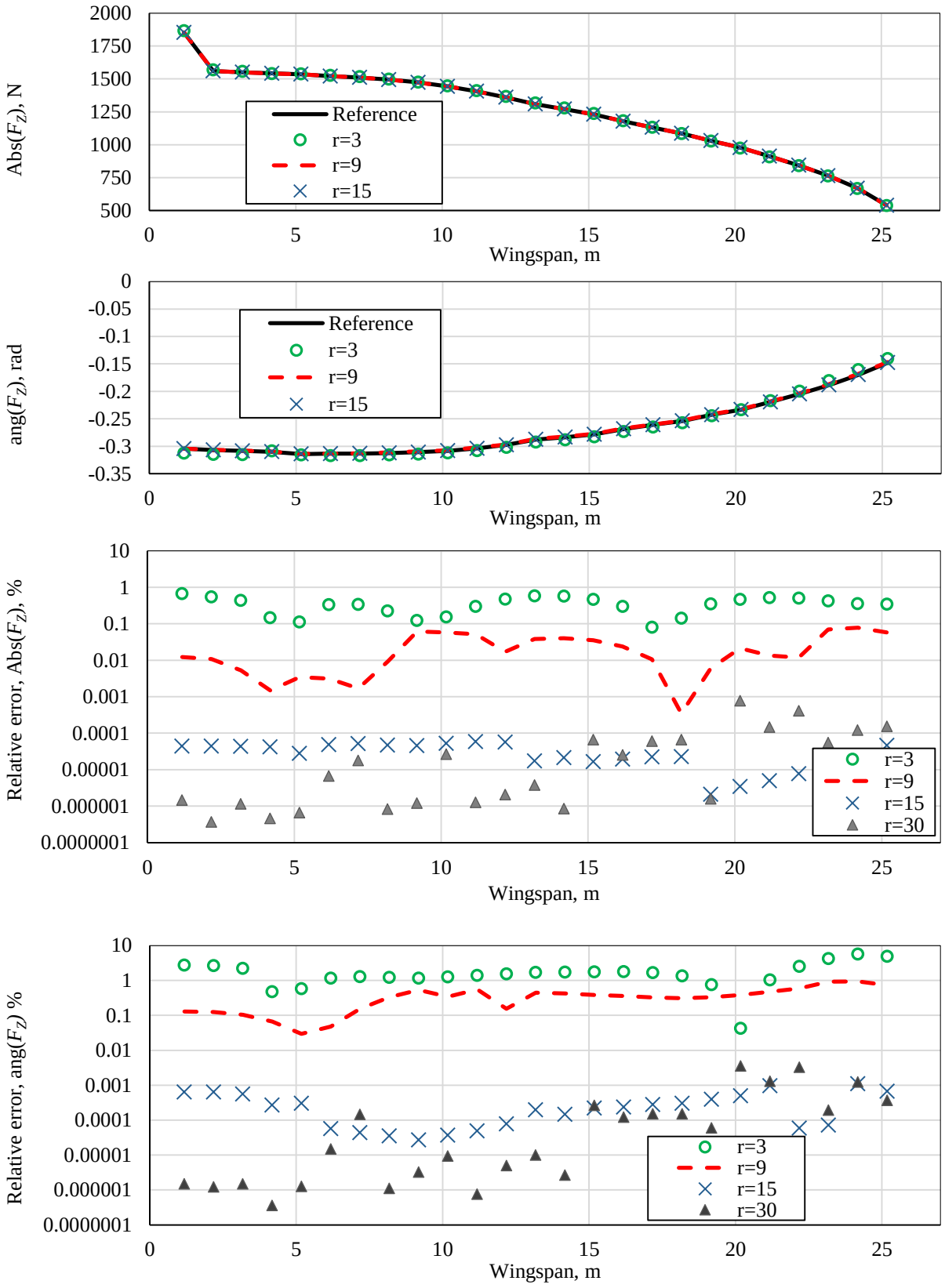

Figure 17: Total F_Z magnitude and phase, with relative error vs ROM size, T=0.02, N=32

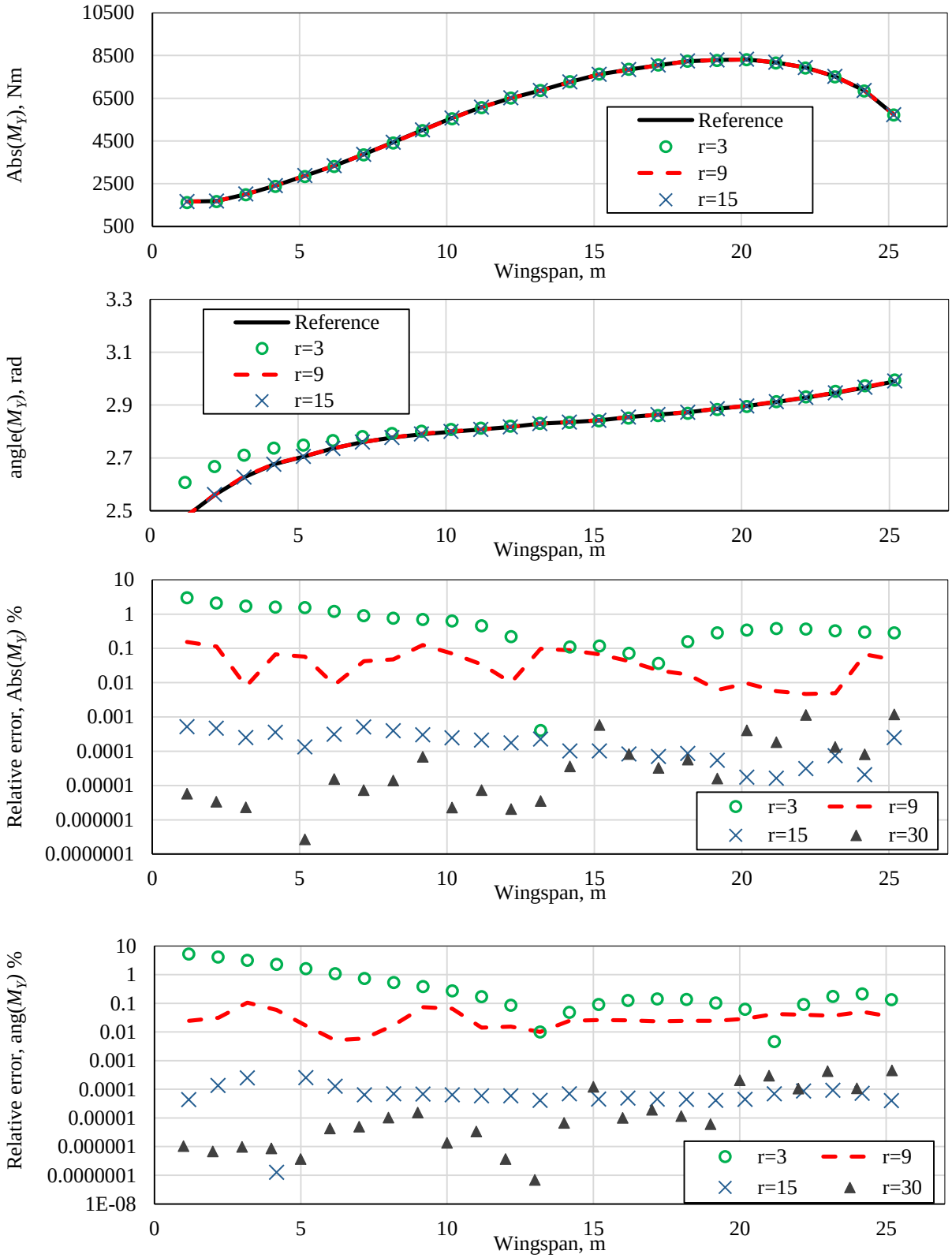

Figure 18: Total M_Y magnitude and phase, with relative error vs ROM size, T=0.02, N=32

Figures 17 and 18 respectively show the ability of the reduced order model to reconstruct the total vertical force and pitching moment on the wing, for one particular frequency (k=0.2). In each case, the reference magnitude and phase of F_Z and M_Y are represented, and can be compared to the prediction given by ROMs of different sizes. Then, the relative error between the reference and the prediction is represented for each ROM size. The ROMs of size 3 are not accurate, particularly when reconstructing the phase of the aerodynamic coefficients. The error in this case is around 1%, with a peak close to 5% close to the wing root. As expected when seeing the errors given by the ROMs on each strip (Figure 16), ROMs of size 9 give a good prediction, with an error between 0.01 and 1% depending on the cases.
But a much better prediction is achieved for r=15, with a relative error in each case lower than 10^{-2} %. Increasing the ROM size to 30 does not improve the accuracy of the model.

V. Conclusions

A reduced order model in the frequency domain has been built and shows a strong ability to reconstruct the frequency response. Applied to a wing, it enables to predict the loads at almost no computational cost. The wing has been sliced in different strips and based on the 2D methodology, reduced order models have been built for the lift and pitching moment for each strip. A sensitivity analysis has been carried out on the optimal choices for the number of inputs needed, the mapping of the continuous frequencies and the ROM size providing the best trade-off between accuracy and efficiency. On each strip or on the whole wing, small ROMs built with only 32 input points enable to reconstruct the frequency response with a maximal error of 0.1%. After having proved its capabilities on a invisicid wing, it is being tested on a viscous mesh.

Acknowledgments

The research leading to these results has received funding from the European Community's Marie Curie Initial Training Network (ITN) on Aircraft Loads Prediction using Enhanced Simulation (ALPES) PEOPLE-ITN-GA-2013-07911. The partners in the ALPES ITN are the University of Bristol, Siemens and Airbus Operations Ltd.

References

[1] P. Eykhoff, "System identification parameter and state estimation," London, Wiley/Interscience, 1974.

[2] G. C. Goodwin, D. J. Hill and M. Palaniswami, "A perspective on convergence of adaptive control algorithms," *Automatica*, vol. 20, no. 5, pp. 519-531, 1984.

[3] L. Ljung, "System identification: theory for the user," *PTR Prentice Hall Information and System Sciences Series*, vol. 198, 1987.

[4] K. J. Åström and B. Wittenmark, Adaptive control, Courier Corporation, 2013.

[5] T. Soderstrom and P. Stoica, System identification, vol. 2, London: Prentice hall, 1989.

[6] M. Kern, "Problèmes inverses," *INRIA, Rocquencourt, BP*, vol. 105, p. 78153, 2002.

[7] W. H. Schilders, H. A. Van der Vorst and J. Rommes, Model order reduction: theory, research aspects and applications, vol. 13, Berlin: Springer, 2008.

[8] Å. Björck, "Solving linear least squares problems by Gram-Schmidt orthogonalization," *BIT Numerical Mathematics*, vol. 7, no. 1, pp. 1-21, 1967.

[9] W. E. Arnoldi, "The principle of minimized iterations in the solution of the matrix eigenvalue problem," *Quarterly of Applied Mathematics,* vol. 9, no. 1, pp. 17-29, 1951.

[10] C. Lanczos, "An iteration method for the solution of the eigenvalue problem of linear differential and integral operators," United States Governm. Press Office, 1950.

[11] Y. Shamash, "Stable reduced-order models using Padé-type approximation," *Automatic Control, IEEE Transactions on,* vol. 19, no. 5, pp. 615-616, 1974.

[12] Z. Bai and R. W. Freund, "A partial Padé-via-Lanczos method for reduced-order modeling," *Linear Algebra and its Applications,* vol. 332, pp. 139-164, 2001.

[13] A. C. Antoulas, "An overview of approximation methods for large-scale dynamical systems," *Annual reviews in Control,* vol. 29, no. 2, pp. 181-190, 2005.

[14] A. Odabasioglu, M. Celik and L. T. Pileggi, "PRIMA : Passive reduced-order interconnect macromodeling algorithm," in *Proceedings of the 1997 IEEE/ACM international conference on Computer-aided design*, IEEE Computer Society, 1997, pp. 58-65.

[15] A. C. Antoulas, Approximation of large-scale dynamical systems, Siam, 2005.

[16] B. Moore, "Principal component analysis in linear systems: Controllability, observability, and model reduction," *Automatic control,* vol. 26, no. 1, pp. 17-32, 1981.

[17] A. M. Lyapunov, "The general problem of the stability of motion," *International Journal of Control,* vol. 55, no. 3, pp. 531-534, 1992.

[18] S. Gugercin and A. C. Antoulas, "A survey of model reduction by balanced truncation and some new results," *International Journal of Control,* vol. 77, no. 8, pp. 748-766, 2004.

[19] D. F. Enns, "Model reduction with balanced realizations: An error bound and a frequency weighted generalization.," in *Decision and Control, 1984. The 23rd IEEE Conference on*, IEEE, 1984, pp. 127-132.

[20] G. Wang, V. Sreeram and W. Q. Liu, "A new frequency-weighted balanced truncation method and an error bound," *IEEE Transactions on Automatic Control,* vol. 44, no. 9, pp. 1734-1737, 1999.

[21] P. Feldmann and R. W. Freund, "Efficient linear circuit analysis by Padé approximation via the Lanczos process," *Computer-Aided Design of Integrated Circuits and Systems, IEEE Transactions on,* vol. 14, no. 5, pp. 639-649, 1995.

[22] J.-N. Juang and R. S. Pappa, "An eigensystem realization algorithm for modal parameter identification and model reduction," *Journal of guidance, control, and dynamics,* vol. 8, no. 5, pp. 620-627, 1985.

[23] G. H. Golub and C. Reinsch, "Singular value decomposition and least squares solutions," *Numerische Mathematik,* vol. 14, no. 5, pp. 403-420, 1970.

[24] T. McKelvey, H. Akçay and L. Ljung, "Subspace-based multivariable system identification from frequency response data," *Automatic Control, IEEE Transactions on,* vol. 41, no. 7, pp. 960-979, 1996.

[25] U. M. Al-Saggaf and G. F. Franklin, "Model reduction via balanced realizations: an extension and frequency weighting techniques," *Automatic Control, IEEE Transactions on,* vol. 33, no. 7, pp. 687-692, 1988.

[26] A. Poncet-Montanges, J. Cooper, D. Jones and Y. Lemmens, "Frequency-domain approach for transonic unsteady aerodynamic modelling," in *SciTech* , San Diego, 2016.

[27] D. Jones and A. Gaitonde, "Future Fast Methods for Loads Calculations: The 'FFAST'Project," *Future,* vol. 3, p. 4, 2012.

[28] D. Schwamborn, T. Gerhold and R. Heinrich, "The DLR TAU-code: Recent applications in research and industry," in *ECCOMAS CFD 2006: Proceedings of the European Conference on Computational Fluid*

Dynamics, Egmond aan Zee, The Netherlands, September 5-8, 2006, Delft University of Technology, European Community on Computational Methods in Applied Sciences (ECCOMAS), 2006.

[29] M. Widhalm, R. P. Dwight, R. Thormann and A. Hübner, "Efficient computation of dynamic stability data with a linearized frequency domain solver," in *European Conference on Computational Fluid Dynamics*, 2010.

[30] P. R. Spalart and S. R. Allmaras, "A one-equation turbulence model for aerodynamic flows, AIAA-92-0439," in *30th aerospace sciences meeting and exhibit*, Reno, NV, 1992.

[31] A. Poncet-Montanges, D. Jones, A.-L. Gaitonde, J. Cooper and Y. Lemmens, "Frequency-domain approach for transonic unsteady aerodynamic modelling," in *IFASD*, Saint Petersburg, 2015.